A Recursive Doubling Dirichlet-to-Neumann Map Method for Periodic Waveguides

Lijun Yuan and Ya Yan Lu*

Abstract

For optical wave-guiding structures composed of uniform segments that are invariant in the longitudinal direction, the Dirichlet-to-Neumann (DtN) map method is highly competitive. Instead of computing the eigenmodes, it calculates the DtN operators of the uniform segments using an efficient Chebyshev collocation scheme. In this paper, a new formulation of the DtN map method is developed for periodic piecewise uniform wave-guiding structures. The method involves a recursive doubling process, so that the overall required computation time is proportional to $\log_2 N$, where N is the number of periods. We illustrate our method by analyzing the scattering of surface plasmon polaritons due to Bragg gratings on metal surfaces and thin metal films.

1 Introduction

Wave-guiding structures that are piecewise uniform in the longitudinal direction are widely used in many optical devices. Numerical simulations are essential to the analysis, design and optimization of these structures. While the finite-difference time-domain (FDTD) method is easy to use, frequency-domain methods that take advantage of the special geometric features of these structures are often more efficient. The most widely used frequency-domain methods [1, 2, 3, 4, 5, 6, 7] rely on eigenmode expansions in each longitudinally uniform segment. The eigenmodes can be calculated semi-analytically [2, 3] for two-dimensional waveguides if the refractive index profile in each segment is piecewise constant, and they can also be calculated numerically, for example, by the finite difference method [4], the finite element method [1], Fourier series [6, 7, 8], etc. An efficient discrete approximation of the continuous spectrum (of the radiation and

*L. Yuan and Y. Y. Lu are with the Department of Mathematics, City University of Hong Kong, Kowloon, Hong Kong. This research was partially supported by a grant from the Research Grants Council of Hong Kong Special Administrative Region, China (Project No. CityU 101706).

evanescent modes) is possible when the perfectly matched layer (PML) [9, 10] technique is used [5, 11]. By calculating the eigenmodes in each segment, discretization of the longitudinal variable is no longer needed.

The bidirectional beam propagation methods (BiBPMs) [12, 13, 14, 15, 16] can also take advantage of the special geometric features of piecewise uniform wave-guiding structures. While conventional beam propagation methods [17] are designed for one-way propagation in slowly varying waveguides, the BiBPMs take into account the multiple reflections at the longitudinal interfaces. In fact, they are extensions of related methods for waveguide junctions [18, 19, 20, 21, 22]. Rational approximations for square root operators and their exponentials are used to efficiently march the directional wave field components in each uniform segment and to analyze the scattering at longitudinal discontinuities. For structures with large longitudinal variations, the non-iterative BiBPMs [13, 15] are more appropriate, since the iterative BiBPMs [12, 16] may fail to converge.

In a recent work [23], we developed a Dirichlet-to-Neumann (DtN) map method for piecewise uniform wave-guiding structures. In each uniform segment, we calculate the DtN operator that maps the wave field at the two ends of the segment to its longitudinal derivative. If the transverse variable is discretized by K points (or K terms are retained in Fourier series expansions), the DtN operator can be approximated by a $(2K) \times (2K)$ matrix. To calculate the DtN operator, we used a Chebyshev collocation method for discretizing the longitudinal variable in the segment. This step requires $O(qK^2)$ operations, where q is the number of points used to discretize the longitudinal variable in the segment. Since the length of a uniform segment is typically smaller than the wavelength, a small value of q (say $q \leq 20$) is sufficient to produce an accurate approximation for the DtN operator. For the eigenmode expansion methods, the longitudinal variable is not discretized, but a large number of eigenmodes must be calculated. If the eigenmodes are calculated numerically [1, 4, 6, 7] and assuming that the transverse operator is discretized by a $K \times K$ matrix and all K eigenvectors are needed, then the required number of operations is $O(K^3)$. Here, the hidden constant in $O(K^3)$ is quite large. For example, multiplying two real $K \times K$ matrices requires about $2K^3$ operations and it takes about 0.4 second for $K = 1000$ on a computer with a Pentium 4 CPU (3.4GHz) in MATLAB. On the contrary, finding all eigenvalues and eigenvectors for a 1000×1000 real tridiagonal matrix requires 37 seconds in the same environment. When the main diagonal of the matrix is complex, the required time is further increased to 58 seconds. Due to the use of PMLs in eigenmode expansion methods [5], the matrix approximating the transverse operator is indeed complex. If the refractive index profile is piecewise constant, the eigenmodes may be calculated by solving a nonlinear equation [2, 3, 5]. When PMLs are used, the eigenvalues are in general complex. It is not an easy task to find all the eigenvalues in a given region of the complex plane from the nonlinear equation. Some

possible approaches are described in [24, 25, 26, 27]. Furthermore, similar to the eigenmode expansion methods, the DtN map method is efficient for wave-guiding structures with many identical segments, since these segments share the same DtN operator.

Comparing with the BiBPMs, the DtN map method is more accurate, since analytic approximations are mostly avoided. The BiBPMs rely on rational approximations to the square root of the transverse operator and the exponential of this square root operator (the one-way propagator). Standard diagonal Padé approximants (both denominator and numerator are polynomials of degree p) for the square root operator and the one-way propagator have exponential convergence for the propagating modes and the radiation modes. That is, the approximation error decreases exponentially as p is increased. But these diagonal Padé approximants fail to approximate the evanescent modes completely. For one-way modeling in slowly varying waveguides, the evanescent modes are not so important and it is sufficient to suppress them [28, 29]. For wave-guiding structures with large longitudinal discontinuities, such as deeply etched waveguide gratings, an accurate modeling of the evanescent modes is necessary. For that purpose, we can use the rotating branch-cut Padé approximation [30] which, however, has a slow convergence. The DtN map method is also more efficient than the BiBPM based on scattering operators [14], since a different and more efficient marching scheme is used. Two operators (approximated by $K \times K$ matrices) are marched from one end of the structure to another giving rise to the solutions of reflected and transmitted waves. If there are m longitudinally uniform segments, the method requires m steps. Each step corresponds to one segment and its DtN map is utilized to march these two operators. The method is sequential, thus the overall computation time is proportional to m.

Piecewise uniform and periodic structures, such as waveguide Bragg gratings, are particularly important in applications. Although the sequential DtN map method [23] can take advantage of the many identical segments by calculating their DtN map only once, it is still not efficient for structures with many periods. In this paper, we develop a recursive doubling process for the DtN map method. The periodicity is utilized to significantly reduce the overall computation time, so that it is proportional to $\log_2 m$. Our recursive doubling process is based on the simple idea of merging DtN maps. It is similar to the recursive doubling process of the scattering operators used in the eigenmode expansion method [5] and the BiBPM [15]. The method is useful when the number of periods is moderate. If the structure has a very large number of periods, the Floquet-Bloch mode expansion technique [4] can be used. For numerical examples, we study a deeply etched waveguide Bragg grating (a modeling task of project COST 268 [36]) and two scattering problems for surface plasmon polaritons involving grating structures on metal surfaces and thin metal films. The surface plasmon polariton problems have been previously analyzed by the Lippmann-Schwinger integral equation method [31] and the

finite-difference time-domain method [32].

2 A DtN operator marching method

For a transverse magnetic (TM) wave propagating in the xz plane, the y-component of the magnetic field, denoted by u here, satisfies

$$\frac{\partial}{\partial z}\left(\frac{1}{\varepsilon}\frac{\partial u}{\partial z}\right)+\frac{\partial}{\partial x}\left(\frac{1}{\varepsilon}\frac{\partial u}{\partial x}\right)+k_0^2\,u=0, \tag{1}$$

where k_0 is the free space wavenumber and $\varepsilon=\varepsilon(x,z)$ is the dielectric function. The time dependence is assumed to be $e^{-i\omega t}$, where ω is the angular frequency. We consider a piecewise z-invariant structure where the longitudinal discontinuities $\{z_j\}$ satisfy $z_0<z_1<...<z_m$. The dielectric function satisfies $\varepsilon=\varepsilon_j(x)$ for $z_{j-1}<z<z_j$ and $0\le j\le m+1$, where $z_{-1}=-\infty$ and $z_{m+1}=\infty$. For such a structure, we assume that an incident wave is given for $z<z_0$ and there are only outgoing waves for $z>z_m$. Our objective is to calculate the reflected wave for $z<z_0$ and the transmitted wave for $z>z_m$.

Using square root operators, we can write down the boundary conditions at $z=z_0^-$ and $z=z_m^+$. In the segment (z_{j-1},z_j), we define a square root operator

$$L_j=\sqrt{\varepsilon_j\partial_x(\varepsilon_j^{-1}\partial_x\ )+\varepsilon_j k_0^2} \tag{2}$$

based on the eigenmodes of the transverse differential operator $\varepsilon_j\partial_x(\varepsilon_j^{-1}\partial_x\ )+\varepsilon_j k_0^2$, such that the forward and backward wave field components in the segment are governed by one-way equations involving L_j. In particular, for $z<z_0$, the incident wave $u^{(i)}$ and the reflected wave $u^{(r)}$ satisfy the following one-way equations

$$\partial_z u^{(i)}=iL_0u^{(i)},\quad \partial_z u^{(r)}=-iL_0u^{(r)}.$$

If we take the z-derivative of the total field $u=u^{(i)}+u^{(r)}$ and eliminate $u^{(r)}$, we obtain the following boundary condition

$$\partial_z u+iL_0u=2iL_0\,u^{(i)}|_{z=z_0^-},\quad z=z_0^-. \tag{3}$$

For $z>z_m$, the transmitted wave is the total wave field. This gives rise to the boundary condition:

$$\partial_z u=iL_{m+1}\,u,\quad z=z_m^+. \tag{4}$$

Since the longitudinal length scale is typically much larger than the wavelength, a number of techniques have been developed to rigorously reduce the boundary value problem (1,3,4) to initial value problems in z using a pair of operators. One approach [33, 34, 23] is to use the operators Q and Y defined at a fixed z by

$$Q(z)u=\varepsilon^{-1}\partial_z u,\quad Y(z)\,u(\cdot,z)=u(\cdot,z_m), \tag{5}$$

where u is an arbitrary solution of (1) and (4). Notice that the operator Q is well defined even at a longitudinal discontinuity z_j. From (4) and the definition of Y, we have

$$Q(z_m) = i\,\varepsilon_{m+1}^{-1} L_{m+1}, \quad Y(z_m) = I, \tag{6}$$

where I is the identity operator. The operators Q and Y satisfy some first order differential equations in z [33]. If they are solved from $z = z_m$ to $z = z_0$, we can then find the reflected and transmitted waves. From (3), we can solve the total field at z_0:

$$[\varepsilon_0 Q(z_0) + iL_0]\, u(x, z_0) = 2iL_0\, u^{(i)}(x, z_0^-). \tag{7}$$

The reflected wave is obtained by subtracting $u^{(i)}$ from u. From the definition of Y, we can calculate the transmitted wave by

$$u(x, z_m) = Y(z_0)\, u(x, z_0). \tag{8}$$

For a piecewise uniform wave-guiding structure, Q and Y can be efficiently marched from z_m to z_0 using DtN maps of the uniform segments [23]. For the segment given by $z_{j-1} < z < z_j$, the DtN map M satisfies

$$M \begin{bmatrix} u(\cdot, z_{j-1}) \\ u(\cdot, z_j) \end{bmatrix} = \begin{bmatrix} M_{11} & M_{12} \\ M_{21} & M_{22} \end{bmatrix} \begin{bmatrix} u(\cdot, z_{j-1}) \\ u(\cdot, z_j) \end{bmatrix} = \begin{bmatrix} \partial_z u(\cdot, z_{j-1}^+) \\ \partial_z u(\cdot, z_j^-) \end{bmatrix} \tag{9}$$

for any solution of (1). Here, the DtN map M has been partitioned as 2×2 blocks. Due to a reflection symmetry, we have $M_{12} = -M_{21}$ and $M_{22} = -M_{11}$. From the continuity conditions of u and $\varepsilon^{-1}\partial_z u$, we can derive the following marching formulas:

$$Z = [\varepsilon_j Q(z_j) - M_{22}]^{-1} M_{21}, \tag{10}$$

$$Q(z_{j-1}) = \varepsilon_j^{-1}(M_{11} + M_{12} Z), \tag{11}$$

$$Y(z_{j-1}) = Y(z_j) Z. \tag{12}$$

When x is discretized by K points, the operators M_{ij}, Q and Y are approximated by $K \times K$ matrices, ε_j and ε_j^{-1} are approximated by diagonal matrices. This step calculates Q and Y at z_{j-1} from those at z_j. The required number of operations is about $(20/3)K^3$. The matrix Z can be obtained in $(8/3)K^3$ operations including $(2/3)K^3$ operations for LU decomposition of the matrix $\varepsilon_j Q(z_j) - M_{22}$ and $2K^3$ operations for solving the columns of Z from the triangular linear systems. Formulas (11) and (12) involve two matrix multiplications that require $4K^3$ operations.

In [23], we developed an efficient Chebyshev collocation method for computing the DtN map M in $O(qK^2)$ operations, where q is the number of points for discretizing (z_{j-1}, z_j) and it is much smaller than K. The method involves the following steps.

1. Discretize z for $z_{j-1} \le z \le z_j$ by

$$\xi_k = z_{j-1} + \frac{z_j - z_{j-1}}{2}\left[1 - \cos\left(\frac{k\pi}{q}\right)\right], \quad k = 0, 1, ..., q.$$

2. Evaluate the differentiation matrix C. The (k, l) entry (for $k, l = 0, ..., q$) of C is

$$c_{kl} = -\frac{2}{z_j - z_{j-1}} \times \begin{cases} (2q^2+1)/6 & \text{if } k = l = 0, \\ -(2q^2+1)/6 & \text{if } k = l = q, \\ -0.5\tau_k/(1-\tau_k^2) & \text{if } 0 < k = l < q, \\ (-1)^{k+l}\sigma_k\sigma_l^{-1}/(\tau_k - \tau_l) & \text{otherwise,} \end{cases}$$

where

$$\tau_k = \cos\left(\frac{k\pi}{q}\right), \quad \sigma_k = \begin{cases} 2 & \text{if } k = 0,\ q \\ 1 & \text{if } 0 < k < q. \end{cases}$$

3. Re-write C and C^2 as

$$C = \begin{bmatrix} c_{00} & \tilde{c}_0 & c_{0q} \\ \vdots & \vdots & \vdots \\ c_{q0} & \tilde{c}_q & c_{qq} \end{bmatrix}, \quad C^2 = \begin{bmatrix} d_{00} & \cdots & d_{0q} \\ \hat{d}_0 & \hat{D} & \hat{d}_q \\ d_{q0} & \cdots & d_{qq} \end{bmatrix},$$

where $\tilde{c}_0$ and $\tilde{c}_q$ are row vectors, $\hat{d}_0$ and $\hat{d}_q$ are column vectors, and $\hat{D}$ is a square matrix.

4. Diagonalize the matrix $\hat{D}$ as

$$\hat{D} = R \begin{bmatrix} \mu_1 & & & \\ & \mu_2 & & \\ & & \ddots & \\ & & & \mu_{q-1} \end{bmatrix} R^{-1}. \tag{13}$$

5. Evaluate column vectors $\vec{\alpha}$ and $\vec{\beta}$, and row vectors $\vec{\gamma}$ and $\vec{\delta}$ by

$$\vec{\alpha} = R^{-1}\hat{d}_0, \quad \vec{\beta} = R^{-1}\hat{d}_q, \quad \vec{\gamma} = \tilde{c}_0 R, \quad \vec{\delta} = \tilde{c}_q R.$$

6. For $k = 1$, 2, ..., $q-1$, solve $w_k(x)$ from

$$\varepsilon_j \frac{d}{dx}\left(\frac{1}{\varepsilon_j}\frac{dw_k}{dx}\right) + (k_0^2\varepsilon_j + \mu_k)w_k = -\alpha_k u(x, z_{j-1}) - \beta_k u(x, z_j). \tag{14}$$

7. Evaluate $\partial_z u$ at z_{j-1}^+ and z_j^- by

$$\partial_z u(x, z_{j-1}^+) = c_{00}u(x, z_{j-1}) + \sum_{k=1}^{q-1}\gamma_k w_k(x) + c_{0q}u(x, z_j), \tag{15}$$

$$\partial_z u(x, z_j^-) = c_{q0}\,u(x, z_{j-1}) + \sum_{k=1}^{q-1}\delta_k w_k(x) + c_{qq}\,u(x, z_j). \tag{16}$$

The first five steps above are preprocessing steps involving the Chebyshev differentiation matrix C [35] and its square. If v is a differentiable function of z for $z_{j-1} \le z \le z_j$, then

$$\begin{bmatrix} v'(\xi_0) \\ v'(\xi_1) \\ \vdots \\ v'(\xi_q) \end{bmatrix} \approx C \begin{bmatrix} v(\xi_0) \\ v(\xi_1) \\ \vdots \\ v(\xi_q) \end{bmatrix},$$

where $\{\xi_k\}$ for $0 \le k \le q$ is a discretization of z and v' is the derivative of v. The most expensive part of these prepossessing steps is the diagonalization of the matrix $\hat{D}$ which requires $O(q^3)$ operations. In the segment (z_{j-1}, z_j), the Helmholtz equation (1) is reduced to

$$\frac{\partial^2 u}{\partial z^2} + \varepsilon_j \frac{\partial}{\partial x}\left(\frac{1}{\varepsilon_j}\frac{\partial u}{\partial x}\right) + k_0^2 \varepsilon_j \, u = 0. \tag{17}$$

Using C^2 to approximate the second order derivative in z, we require that (17) is valid at ξ_k for $1 \le k \le q-1$. When $\hat{D}$ is diagonalized, these equations are transformed to $q-1$ separate ordinary differential equations given in (14), where

$$\begin{bmatrix} w_1(x) \\ w_2(x) \\ \vdots \\ w_{q-1}(x) \end{bmatrix} = R^{-1} \begin{bmatrix} u(x,\xi_1) \\ u(x,\xi_2) \\ \vdots \\ u(x,\xi_{q-1}) \end{bmatrix}.$$

In steps 6 and 7, we calculate $\partial_z u$ at z_{j-1}^+ and z_j^- assuming that u is given at z_{j-1} and z_j. If a finite difference or finite element method is used to discretize x with K points, Eq. (14) for a single w_k can be solved in $O(K)$ operations. Therefore, $O(qK)$ operations are required for step 6. Clearly, step 7 also requires $O(qK)$ operations. To calculate the DtN map M, steps 6 and 7 must be repeated for K times. From the definition of M given in (9), we observe that a column of M can be obtained if $u(x, z_{j-1})$ and $u(x, z_j)$ (discretized as column vectors) are taken as a column vector of the $(2K) \times (2K)$ identity matrix. Due to the reflection symmetry, we only have to go through the first K columns of the $(2K) \times (2K)$ identity matrix. Therefore, the DtN map M can be found in $O(qK^2)$ operations. Since Eq. (14) is solved repeatedly for K different right hand sides, additional saving is possible by calculating the LU decomposition of the matrix (approximating the differential operator at the left hand side of (14)) only once. Overall, computing the DtN map M is much easier than computing the eigenvalue decomposition of the transverse operator.

3 A recursive doubling process

Instead of marching two operators Q and Y, an alternative approach is to find the DtN map G of the entire non-uniform part of the structure given by $z_0 < z < z_m$. The

operator G maps u at z_0 and z_m to $\partial_z u$ at z_0^+ and z_m^-. Once G is obtained, it is easy to find the reflected and transmitted waves. In fact, using the boundary conditions (3) and (4) and writing down the operator G in a 2×2 block matrix form, we obtain the following system for the wave field at z_0 and z_m:

$$\begin{bmatrix} G_{11} + i\rho_0^{-1} L_0 & G_{12} \\ G_{21} & G_{22} - i\rho_m L_{m+1} \end{bmatrix} \begin{bmatrix} u(\cdot, z_0) \\ u(\cdot, z_m) \end{bmatrix} = \begin{bmatrix} 2i\rho_0^{-1} L_0 u^{(i)}(\cdot, z_0^-) \\ 0 \end{bmatrix}, \tag{18}$$

where $\rho_0 = \varepsilon_0/\varepsilon_1$ and $\rho_m = \varepsilon_m/\varepsilon_{m+1}$. The two square root operators L_0 and L_{m+1} can be approximated using a rotating branch-cut Padé approximant [30] as in the BiBPMs [13, 15].

To find the global DtN map G, we need a merging process that computes the DtN map of the segment $a < z < c$ from the DtN maps of the segments $a < z < b$ and $b < z < c$. Let us denote the DtN maps of these segments by U, V and W, respectively. The operator U satisfies an equation as (9), but with z_{j-1} and z_j replaced by a and b, respectively. The equations for V and W are similar. With U and V partitioned as 2×2 blocks and using the continuities of u and $\varepsilon^{-1}\partial_z u$ at $z = b$, we can eliminate $u(\cdot, b)$ and obtain

$$[K_1, K_2] = (U_{22} - \rho V_{11})^{-1}[U_{21}, \rho V_{12}], \tag{19}$$

$$W = \begin{bmatrix} U_{11} - U_{12}K_1 & U_{12}K_2 \\ -V_{21}K_1 & V_{21}K_2 + V_{22} \end{bmatrix}, \tag{20}$$

where $\rho(x) = \varepsilon(x, b^-)/\varepsilon(x, b^+)$. For a general piecewise uniform structure, we can start a recursion for $j = 2, 3, ..., m$. For the j-th step, we use the above merging formulas to find the DtN map of the segment (z_0, z_j) from the DtN maps of segments (z_0, z_{j-1}) and (z_{j-1}, z_j). After the recursion is completed, we obtain the global DtN map G.

If the structure is periodic, G can be more efficiently calculated. Starting from the DtN map for one period, we use the merging formulas recursively to find the DtN maps for 2 periods, 4 periods, etc. In general, we calculate the DtN map for 2^{l+1} periods from the DtN map for 2^l periods. If the structure contains N periods, we expand the integer N in its binary form, say $(r_k ... r_2 r_1 r_0)_2$, then merge the DtN map for 2^l period if $r_l = 1$. For example, the binary form of 22 is $(10110)_2$, then the DtN map for 22 periods is obtained from merging the DtN maps of 2 periods, 4 periods and 16 periods. Clearly, the required number of operations is proportional to $\log_2 N$.

Next, we consider a periodic piecewise uniform structure obtained by modifying a straight waveguide. The dielectric function profile of the original waveguide is ε_0. The structure has N modified segments each having a length l_1 and a dielectric function profile ε_1. Between the modified segments, there are $N - 1$ segments of length l_0 corresponding to the original waveguide. The structure has $2N$ longitudinal discontinuities $\{z_0, z_1, ..., z_{2N-1}\}$ satisfying

$$z_{2j} = z_0 + j(l_0 + l_1), \quad z_{2j+1} = z_{2j} + l_1 \quad \text{for} \quad j = 0, 1, ..., N - 1.$$

The dielectric functions of the uniform segments satisfy $\varepsilon_{2j} = \varepsilon_0$ and $\varepsilon_{2j+1} = \varepsilon_1$. This structure is (partially) periodic with period $l_0 + l_1$. For convenience, we let $m = 2N$ and introduce an extra point z_m such that $z_0 < z < z_m$ contains exactly N periods. Since z_m is not a longitudinal discontinuity, we have $\varepsilon_{m+1} = \varepsilon_{2N+1} = \varepsilon_0$. For this structure, there are two DtN maps $M^{(0)}$ and $M^{(1)}$ corresponding to the uniform segments with dielectric functions ε_0 and ε_1, respectively. There two DtN maps are merged to obtain the DtN map for one period, such as (z_0, z_2). The recursive doubling process is then used to find the global DtN map G for the entire structure (i.e. $z_0 < z < z_m$).

4 Numerical examples

In this section, we consider three examples. The first example is a modeling task of the COST 268 project [36] and it is used to validate the recursive doubling DtN map method developed in this paper. The other two examples [31, 32] are Bragg gratings of surface plasmon polariton (SPP) waveguides. SSPs are being extensively studied due to their potential applications in sub-wavelength photonic devices.

The structure considered by the COST 268 project [36] is a deeply etched short Bragg grating in a high contrast optical waveguide. The waveguide is formed by a $0.5\,\mu m$ Si_3N_4 layer on a SiO_2 substrate. Refractive indices of the waveguide core and the substrate are given in [36]. For the TM polarization, we follow Čtyroký [7] and consider a 20 period grating formed by grooves with a pitch of $0.23\,\mu m$ and a duty cycle of $1:1$ (i.e., $l_0 = l_1 = 0.23\,\mu m$) deeply etched into the guiding layer with the etching depth $0.75\,\mu m$. For the x variable, we use a computation window of $5.5\,\mu m$ ($3\,\mu m$ for the substrate and $2\,\mu m$ for the air cladding), and discretize it by 441 points. PMLs of 20 grid points are used at both ends of the x interval. The DtN maps of each uniform segments are calculated with 20 points in the z direction. In Fig. 1, we show the transmittance and reflectance of the fundamental TM mode of the original straight waveguide. For comparison, we also show the results of Čtyroký [7] obtained using an eigenmode expansion method based on Fourier sine series. It is clear that the two methods are in good agreement.

Next, we use this example to study the accuracy of the DtN map method and the BiBPM [15]. For simplicity, this is considered only at a fixed free space wavelength $\lambda = 1.25\,\mu m$. A reference solution is obtained by a finite difference eigenmode expansion method (FD-EEM) [4]. Assuming that these three methods use the same finite difference scheme to discretize the transverse operator, the FD-EEM is the most accurate, since it rigorously computes the forward and backward wave field components based on eigenvalue decompositions. The BiBPM introduces errors due to rational approximations to the square root operator L_j given in (2) and its exponential $P_j = \exp[i(z_j - z_{j-1})L_j]$ for each segment. The DtN map method requires only approximations to L_0 and L_{m+1} in

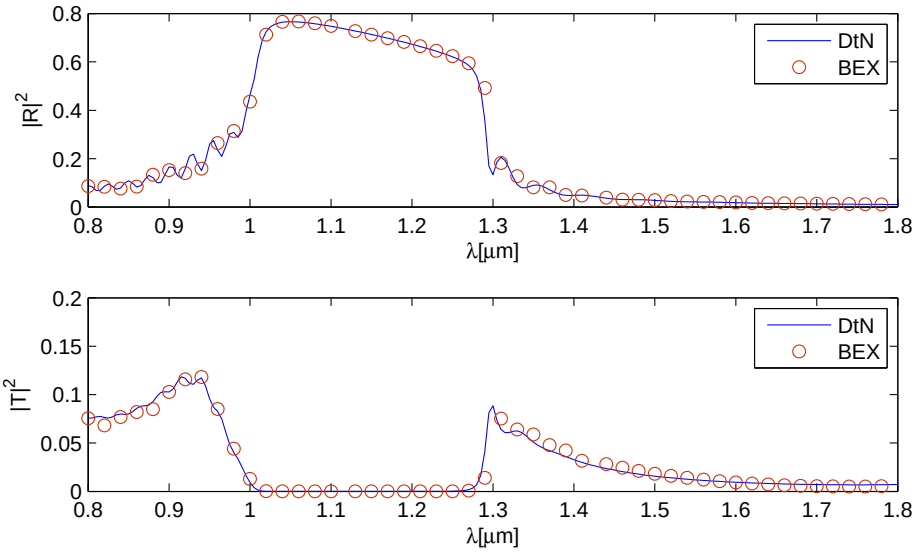

Figure 1: Reflectance and transmittance of the fundamental TM mode for a deeply etched optical waveguide grating with 20 periods. The solid lines and the small circles are the results of the DtN map method and the eigenmode expansion method based on Fourier sine series [7].

the boundary conditions (3) and (4), but it also introduces additional errors when the longitudinal variable z is discretized by the Chebyshev collocation method. For a square root operator, we use the $[p/p]$ Padé approximant with the branch-cut rotated by an angle θ. A rational approximation of P_j is obtained by first inserting the approximation of L_j and then applying the $[r/r]$ Padé approximation of the exponential function. We fix $\theta = \pi/6$, $r = 2$ and consider $p = 4$ and $p = 5$. Using a small grid size $\Delta x = 0.00625\,\mu m$ and a total of 881 grid points for the x variable, we obtain approximate values of the reflection coefficient R_f, R_d and R_b by the FD-EEM method, the DtN map method and the BiBPM, respectively. In particular, FD-EEM gives a reflectance of $|R_f|^2 = 0.62171$. Another calculation with an even smaller grid size indicates that R_f is accurate to 3 or 4 digits. To analyze the additional errors of the DtN map method and the BiBPM, we use R_f as the reference solution and calculate the relative errors of $|R_d|^2$ and $|R_b|^2$, defined as $\mathrm{RE}_d = ||R_d|^2 - |R_f|^2|/|R_f|^2$ and $\mathrm{RE}_b = ||R_b|^2 - |R_f|^2|/|R_f|^2$. The results are given in Table 1. We observe that the DtN map method is more accurate than the BiBPM.

p	RE_b	RE_d
4	1.5×10^{-3}	1.5×10^{-4}
5	3.2×10^{-3}	9.0×10^{-5}

Table 1: Relative errors of $|R|^2$ for the BiBPM and DtN map method.

The second example has been analyzed earlier by Søndergaard *et al.* [31]. The structure, as shown in Fig. 2, is a thin gold film with gold ridges surrounded by a polymer

Figure 2: Schematic view of a long range SPP waveguide Bragg grating structure.

with refractive index 1.543. The thickness of the gold film is $d_0 = 15\,\text{nm}$. The ridges appear in both sides of the thin film and they have a height of $h = 10\,\text{nm}$ and a length of $l_1 = 230\,\text{nm}$. The segments between the ridges have a constant length of $l_0 = 270\,\text{nm}$. The grating period is thus $l_0 + l_1 = 500\,\text{nm}$. In the following, we calculate the reflection and transmission spectra for three cases corresponding to $N = 80$, 160 and 320, where N is the number of ridges. The incident field is the fundamental mode of the plasmon waveguide with the 15 nm gold core. We calculate the reflection and transmission coefficients, R and T, defined as the coefficients of the fundamental mode when the reflected and transmitted fields are expanded. If we assume that the fundamental mode of the SPP waveguide has unit power at the left side of the first ridge (i.e. $z = 0$), then $|T|^2$ represents the power carried by the same mode at the right side of the last ridge (i.e. $z = Nl_1 + (N-1)l_0$). For simplicity, we assume a constant refractive index $n = 0.559 + 9.81i$ for gold. This is a reasonable approximation for wavelength from $1.52\,\mu m$ to $1.58\,\mu m$ [37]. Our results, as well as those reported in [31], are shown in Fig. 3. In fact, Søndergaard *et al.* [31] evaluated the transmittance at $z = N(l_0+l_1)+5\mu m$. This partially explains the difference between the transmittance results in Fig. 3. In our calculations, we have used a second order finite difference scheme to approximate the transverse operator. The x variable is discretized by 647 points using a non-uniform mesh where the grid size varies from 2.5 nm to 97 nm. The computation window is about $51\,\mu$m including a PML of 20 grid points in each side of the structure. The DtN maps of the two distinct uniform segments are calculated by the Chebyshev collocation method using only 10 points in the z direction. The square root operators L_0 and L_{m+1} in the boundary conditions (3) and (4) are approximated by a rotating branch-cut Padé approximation with $p = 7$ and $\theta = \pi/6$.

As the third example, we consider the metal-insulator-metal Bragg grating structure proposed and analyzed by Han *et al.* [32]. As shown in Fig. 4, the original straight SPP waveguide is an air gap of width $d_0 = 100\,\text{nm}$ between two silver layers. A grating structure is created by introducing N identical segments where the width of the air gap is symmetrically increased to $d_1 = 150\,\text{nm}$. Between these N segments with wider air gaps, there are $N - 1$ segments identical to the original waveguide. The lengths of segments

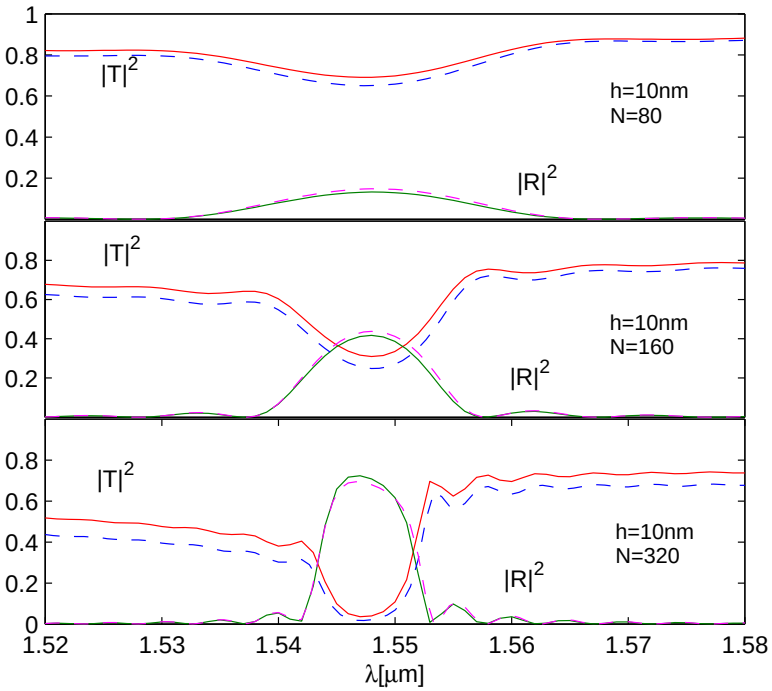

Figure 3: Reflectance $|R|^2$ and transmittance $|T|^2$ for a surface plasmon polariton Bragg grating with a 15 nm gold film and N symmetric gold ridges of height $h = 10$ nm. The solid and dashed lines correspond to the DtN map method and the integral equation method [31], respectively.

Figure 4: Schematic view of a metal-insulator-metal SPP Bragg grating structure.

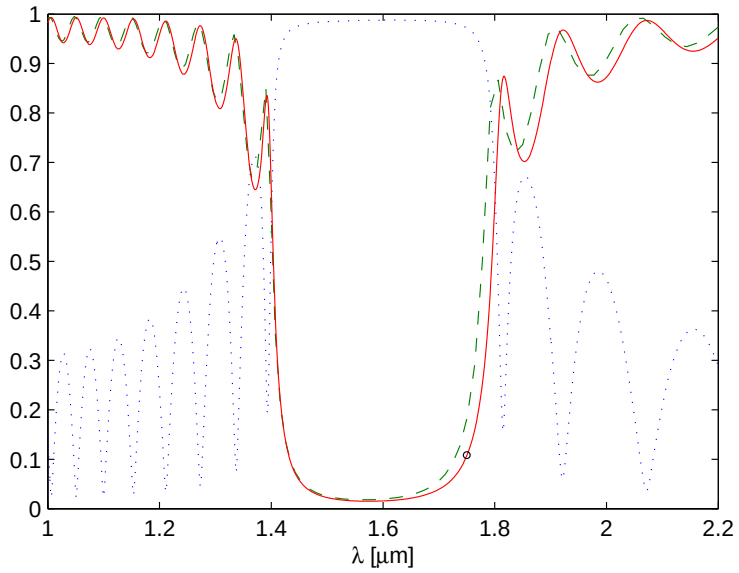

Figure 5: Transmission and reflection spectra of a metal-insulator-metal waveguide Bragg grating with $N = 14$ periods. The dashed line is the magnitude of the scaled transmission coefficient (i.e., $|T_s|$) of Han *et a.* [32]. The solid and dash-dot lines are the magnitudes of the scaled transmission and reflection coefficients (i.e. $|T_s|$ and $|R|$) calculated by the DtN map method. For $\lambda = 1.75\,\mu m$, a more accurate solution is shown as the little circle.

with wide and narrow air gaps are $l_1 = 292\,\text{nm}$ and $l_0 = 368\,\text{nm}$, respectively. The grating period is thus 660 nm. As in [32], we use a simple Drude model for the dielectric function of silver and consider two cases for $N = 14$ and $N = 17$. Using the fundamental mode of the original straight waveguide as the incident field, we obtain the transmission and reflection spectra in Fig. 5 and Fig. 6 for $N = 14$ and $N = 17$, respectively. The scaled transmission coefficient T_s is defined as $T_s = T \exp[\sigma_1 N l_1 + \sigma_0 (N-1) l_0]$, where σ_j (for $j = 0$ or 1) is the imaginary part of the propagation constant of the fundamental mode in the segment with the air gap width d_j. The FDTD results [32] for the scaled transmission coefficient are also shown in Fig. 5 and Fig. 6, as the dashed lines. As far as the main features are concerned, our results agree with those of Han *et al.* [32]. However, the two solutions do not agree so well for large wavelengths. Our results are obtained using a computation window of $1\,\mu m$ and 201 discrete points in the transverse direction. The DtN maps of the two uniform segments are calculated by the Chebyshev collocation method using 15 points in the z direction. The square root operators L_0 and L_{m+1} in the boundary conditions (3) and (4) are approximated by a rotating branch-cut Padé approximation with $p = 7$ and $\theta = \pi/6$. To validate our result, we fix the wavelength at $\lambda = 1.75\,\mu m$ and the number of period at $N = 14$, increase the computation window to $2\,\mu m$ and decrease the grid size in the x direction by one half, so that the total number of

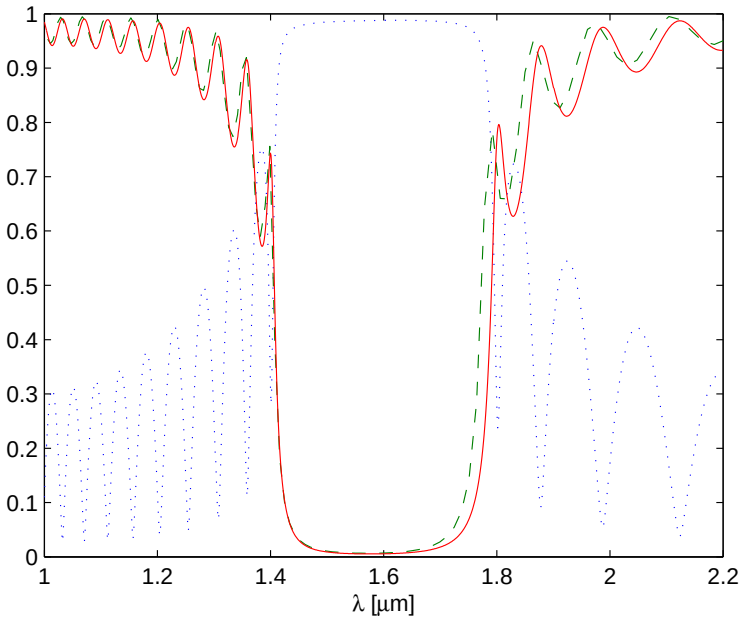

Figure 6: Same as Fig. 5, except that the number of period is $N = 17$.

points in the x direction is now 801. The transmission coefficient is then calculated by the finite difference eigenmode expansion method. We obtain $|T_s| \approx 0.1082$ for $\lambda = 1.75\mu m$. As indicated by the little circle in Fig. 5, this accurate result agrees with our earlier result based on the recursive doubling DtN map method, a coarser grid and a smaller computation window.

5 Conclusion

We have developed a recursive doubling Dirichlet-to-Neumann (DtN) map method for piecewise uniform and periodic wave-guiding structures. The method makes use of the DtN operators of the uniform segments. These operators can be efficiently calculated by a Chebyshev collocation method. The recursive doubling process is based on the merging of DtN maps and it allows us to reduce the computation time from proportional to N to proportional to $\log_2 N$, where N is the number of periods. Compared with the eigenmode expansion method [5] and the BiBPM [15], where a recursive doubling process for the scattering operators is used, the DtN map method is highly competitive, because we do not need the time-consuming step of calculating the eigenmodes and analytic approximations used in BiBPMs are mostly avoided. The method is developed for two-dimensional waveguide structures. We believe it is possible to extend the method to three-dimensional piecewise uniform structures. For that, we need a high order discretization of the transverse operator and to take care of the full vector nature.

Our method is used to compute the transmission and reflection spectra for a deeply etched waveguide Bragg grating (a modeling task of COST 268 project) and two surface plasmon polariton waveguide Bragg grating structures. Numerical results for the first example are in good agreement with those reported in [7]. For the two SPP waveguide grating structures, our numerical results are quite close to the earlier FDTD [32] and integral equation [31] results.

Acknowledgments

The authors sincerely thank Prof. J. Čtyroký, Dr. T. Søndergaard, Dr. Z. Han and other authors of [31] and [32] for providing us the data for comparison and for their patience and time to explain their research to us.

References

[1] Q. H. Liu and W. C. Chew, "Analysis of discontinuities in planar dielectric waveguides: an eigenmode propagation method", *IEEE Transactions on Microwave Theory and Techniques*, Vol. 39(3), pp. 422-430, March 1991.

[2] G. Sztefka and H. P. Nolting, "Bidirectional eigenmode propagation for large refractive index steps", *IEEE Photonics Technology Letters*, Vol. 5, pp. 554-557, 1993.

[3] J. Willems, J. Haes and R. Baets, "The bidirectional mode expansion method for 2-dimensional wave-guides - the TM case", *Optical and Quantum Electronics*, 27(10): 995-1007, Oct 1995.

[4] S. F. Helfert and R. Pregla, "Efficient analysis of periodic structures", *Journal of Lightwave Technology*, Vol. 16, pp. 1694-1702, Sept. 1998.

[5] P. Bienstman and R. Baets, "Optical modelling of photonic crystals and VCSELs using eigenmode expansion and perfectly matched layers", *Opt. Quant. Electron.*, Vol. 33, pp. 327-341, April 2001.

[6] E. Silberstein, P. Lalanne, J. P. Hugonin and Q. Cao, "Use of grating theories in integrated optics", *J. Opt. Soc. Am. A*, Vol. 18, pp. 2865-2875, Nov. 2001.

[7] J. Čtyroký, "A simple bi-directional mode expansion propagation algorithm based on modes of a parallel-plate waveguide", *Optical and Quantum Electronics*, 38 (1-3): 45-62, Jan. 2006.

[8] J. Čtyroký, "Improved bidirectional mode expansion propagation algorithm based on Fourier series", to appear in *Journal of Lightwave Technology*.

[9] J. P. Berenger, "A perfectly matched layer for the absorption of electromagnetic-waves", *J Comput Phys*, 114(2): 185-200, 1994.

[10] W. C. Chew and W. H. Weedon, "A 3D perfectly matched medium from modified Maxwells equations with stretched coordinates", *Microwave and Optical Technology Letters*, 7(13): 599-604, 1994.

[11] F. Olyslager, "Discretization of continuous spectra based on perfectly matched layers", *SIAM Journal on Applied Mathematics*, 64 (4): 1408-1433, 2004.

[12] H. Rao, R. Scarmozzino and R. M. Osgood, "A bidirectional beam propagation method for multiple dielectric interfaces", *IEEE Photonics Technology Letters*, Vol. 11, No. 7, pp. 830-832, 1999.

[13] H. El-Refaei, D. Yevick and I. Betty, "Stable and noniterative bidirectional beam propagation method", *IEEE Photonics Technology Letters*, Vol. 12, pp. 389-391, 2000.

[14] P. L. Ho and Y. Y. Lu, "A stable bidirectional propagation method based on scattering operators", *IEEE Photon. Technol. Lett.*, Vol. 13, No. 12, pp. 1316-1318, 2001.

[15] P. L. Ho and Y. Y. Lu, "A bidirectional beam propagation method for periodic waveguides", *IEEE Photon. Technol. Lett.*, Vol. 14, pp. 325-327, March 2002.

[16] Y. Y. Lu and S. H. Wei, "A new iterative bidirectional beam propagation method", *IEEE Photonics Technology Letters*, Vol. 14, No. 11, pp. 1533-1535, Nov. 2002.

[17] J. Yamauchi, *Propagating Beam Analysis of Optical Waveguides*, Research Studies Press, UK, 2003.

[18] Y. P. Chiou and H. C. Chang, "Analysis of optical waveguide discontinuities using the Padé approximations", *IEEE Photon. Technol. Lett.*, Vol. 9, pp. 946-966, 1997.

[19] C. Yu and D. Yevick, "Application of the bidirectional parabolic equation method to optical waveguide facets", *J. Opt. Soc. Am. A*, Vol. 14, No. 7, pp. 1448-1450, 1997.

[20] H. El-Refaei, I. Betty and D. Yevick, "The application of complex Padé approximants to reflection at optical waveguide facets", *IEEE Photon. Technol. Lett.*, vol. 12, no. 2, Feb. 2000.

[21] S. H. Wei and Y. Y. Lu, "Application of Bi-CGSTAB to waveguide discontinuity problems", *IEEE Photon. Technol. Lett*, Vol. 14, pp. 645-647, 2002.

[22] N. N. Feng and W. P. Huang, "A field-based numerical method for three-dimensional analysis of optical waveguide discontinuities", *IEEE J. Quantum Electronics*, Vol. 39, pp. 1661-1665, Dec. 2003.

[23] L. Yuan and Y. Y. Lu, "An efficient bidirectional propagation method based on Dirichlet-to-Neumann maps", *IEEE Photonics Technology Letters*, Vol. 18, pp. 1967-1969, Sept. 2006.

[24] R.Z.L. Ye and D. Yevick, "Noniterative calculation of complex propagation constants in planar waveguides", *Journal of the Optical Society of America A*, 18(11): 2819-2822, 2001.

[25] S. B. Gaal, H. J. W. M. Hoekstra, P. V. Lambeck, "Determining PML modes in 2-D stratified media", *Journal of Lightwave Technology*, 21(1): 293-298, Jan. 2003.

[26] H. Rogier, L. Knockaert and D. De Zutter, "Fast calculation of the propagation constants of leaky and Berenger modes of planar and circular dielectric waveguides terminated by a perfectly matched layer", *Microwave and Optical Technology Letters*, 37 (3): 167-171, May 2003.

[27] L. Knockaert, H. Rogier and D. De Zutter, "An FFT-based signal identification approach for obtaining the propagation constants of the leaky modes in layered media", *AEU-International Journal of Electronics and Communications*, 59(4): 230-238, 2005.

[28] Y. Y. Lu, A complex coefficient rational approximation of $\sqrt{1+x}$, *Applied Numerical Mathematics*, Vol. 27(2), pp. 141-154, 1998.

[29] Y. Y. Lu and P. L. Ho, Beam propagation method using a $[(p-1)/p]$ Padé approximant of the propagator, *Optics Letters*, Vol. 27, No. 9, pp. 683-685, May 2002.

[30] F. A. Milinazzo, C. A. Zala and G. H. Brooke, Rational square-root approximations for parabolic equation algorithms, *J. Acoust. Soc. Am.*, 101(2), pp. 760-766, 1997.

[31] T. Søndergaard, S. I. Bozhevolnyi and A. Boltasseva, "Theoretical analysis of ridge gratings for long-range surface plasmon polartions", *Physical Review B*, Vol. 73, 045320, 2006

[32] Z. Han, E. Forsberg and S. He, "Surface plasmon Bragg gratings formed in metal-insulator-metal waveguides", *IEEE Photonics Technology Letters*, Vol. 19, pp. 91-93, Jan. 2007.

[33] Y. Y. Lu and J. R. McLaughlin, "The Riccati method for the Helmholtz equation", *Journal of the Acoustical Society of America,* Vol. 100(3), p.1432-1446, 1996.

[34] Y. Y. Lu, "One-way large range step methods for Helmholtz waveguides", *Journal of Computational Physics*. Vol 152(1), pp. 231-150, 1999.

[35] L. N. Trefethen, *Spectral Methods in MATLAB*, Society for Industrial and Applied Mathematics, 2000.

[36] J. Čtyroký, S. Helfert, R. Pregla, *et al.* "Bragg waveguide grating as a 1D photonic band gap structure: COST 268 modelling task", *Optical and Quantum Electronics*, Vol. 34, pp. 455-470, 2002.

[37] E. D. Palik, *Handbook of Optical Constants of Solids*, Academic Press, Orlando, 1985.